COMPUTER EVALUATION OF EXCHANGE FACTORS IN THERMAL RADIATION

REDHOUANE HENDA
Laurentian University • Sudbury, Ontario, Canada P3E 2C6

Computer software packages that supplement traditional classroom presentations can provide opportunities in reflection and action to students.[1-4] A key factor for successful development and use of computer packages in engineering education is identification of activities that cannot be accomplished by other means, *e.g.,* analytically. Such is the case for most thermal radiation problems.

Thermal radiation is offered as part of heat transfer courses in all chemical engineering programs, although not as intensively as in their mechanical engineering counterparts. At least two aspects are very peculiar to thermal radiation transfer compared to other modes of transport. First, the mechanism of thermal radiation has no analogy in momentum and mass transport—a very useful tool in the instruction of the different modes of transport. Second, the equations of heat transfer by radiation are strongly nonlinear, making it difficult to solve radiation problems using analytical or even numerical techniques, especially for complex geometries and/or real surfaces.

In evaluating any thermal radiation exchange, it is fundamental to calculate the view or exchange factors. Generally, the instruction of thermal radiation to chemical engineers revolves around a thorough understanding of the properties of the view factor and of the tools to evaluate it. For simple geometries, view factors have been evaluated and tabulated in catalogues.[5,6] For moderately involved geometries, however, view factors are exceedingly difficult to evaluate analytically. Different numerical techniques, such as the finite element method, area and line integral methods, and the Romberg formula, were used to compute the view factor.[7-9] More often than not, statistical approaches, such as the Monte Carlo (MC) technique, are the only alternative.

An advantage of the MC technique is its ability to tackle the most complicated problems with relative ease. It also allows for a better analysis of the design parameters that affect distribution of thermal patterns arising from thermal radiation exchange in realistic geometries in an effort, for instance, to optimize these parameters. Its disadvantage lies in the issue of accuracy of the results, although statistical errors can be resolved through an increase in sample size and an adequate choice of a random number generator.

This paper describes a computer program that serves as an educational tool in the instruction of the notion of view factor in a nontrivial geometry using the MC technique. The concept of exchange factor, which induces the effect of multiple reflections, is also considered in detail. Thermal radiation occurs between discrete sources (both a single source and a linear succession of sources are considered) and the walls of a rectangular enclosure containing an obstructing surface. All surfaces are separated by a transparent medium and are assumed to be isothermal with uniform properties. The surfaces can be black, diffuse-grey, or diffuse-nongray. The discrete sources are black bodies emitting at a high temperature (T = 2700K). In order to make the problem tractable at the undergraduate level, the surfaces are assumed to be cool enough so their emission can be neglected.

MODELING

The enclosure considered is a box with six sides and obstructing surface as sketched in Figure 1a. Thermal radiation is emitted by discrete isotropic sources in the form of energy bundles that travel along straight paths through the enclosure until they are absorbed by a surface or terminated after a preset, high-enough number of reflections on the surfaces. Solving exchanged thermal radiation using the MC technique necessitates tracing the history of randomly sampled photons from their point of emission to their point of absorption or

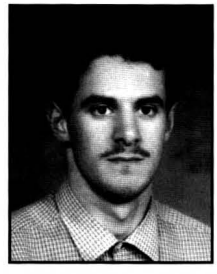

***Redhouane Henda** is Associate Professor in the School of Engineering at Laurentian University (Canada). He received his MSc and PhD degrees in chemical engineering from l'Institut de Génie Chimique and LAAS-CNRS (France), and is a recipient of the Alexander von Humboldt foundation (Germany). Presently, he teaches courses related to transport phenomena, numerical analysis, and materials engineering. His current research interests include dynamical chemical systems, advanced materials, and engineering education.*

attenuation, after simple or multiple reflections. A photon history is tracked using a ray-tracing approach[10] (as shown in Figure 1b) relative to enclosure and source systems of coordinates. In order to follow the history of energy bundles in a statistically sound way, the position and properties of bundles are chosen according to probability distributions. The fraction of energy emitted over wavelengths between 0 and λ is expressed by[11]

$$R(\lambda) = \int_0^{\lambda} P(\lambda)d\lambda = \frac{\int_0^{\lambda} E_\lambda d\lambda}{\int_0^{\lambda} E_\lambda d\lambda} \qquad (1)$$

Equation (1) is then inverted to correctly model a specific bundle property. In case of a single source, the position of the latter in the enclosure is rather deterministic. For the case of a uniform linear succession of discrete sources, based on Eq.

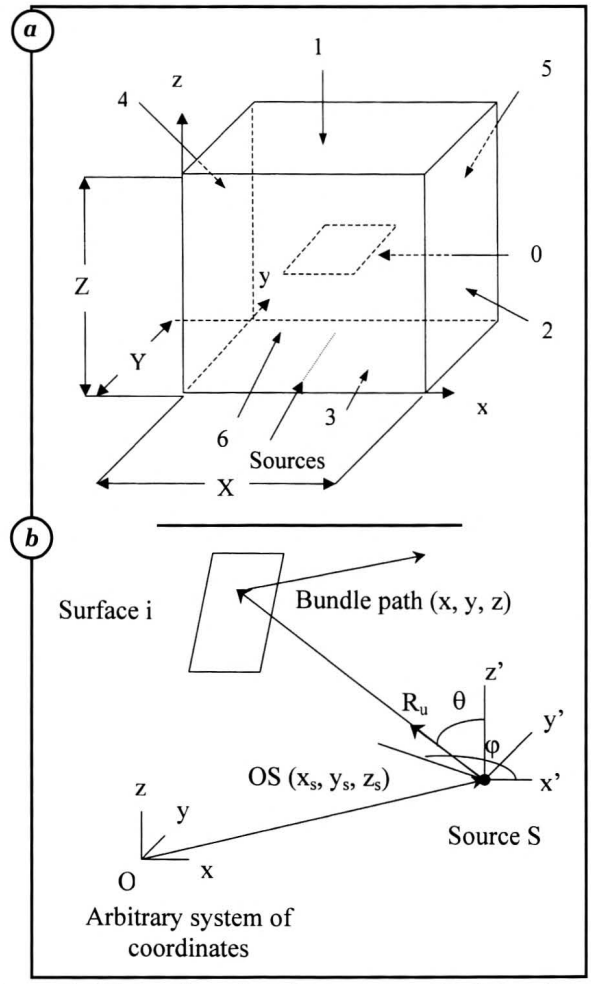

Figure 1. *Schematics of enclosure geometry (a) and vector description of an energy bundle (b). The dimensionless depth and height of the enclosure are Y/S = 1 and Z/X = 1 (with X = 20 cm), respectively, and the dimensions of the obstructing surface are 10 x 10 cm².*

(1) a source position (x_s, y_s, z_s) is chosen randomly along a linear segment of coordinates ($x_{sg,1}$, $y_{sg,1}$, $z_{sg,1}$) and $x_{sg,2}$, $y_{sg,2}$, $z_{sg,2}$), as follows:

$$\begin{aligned} x_s &= (1 - R_s)x_{sg,1} + R_s x_{sg,2} \\ y_s &= (1 - R_s)y_{sg,1} + R_s y_{sg,2} \\ z_s &= (1 - R_s)z_{sg,1} + R_s z_{sg,2} \end{aligned} \qquad (2)$$

where R_s is a number between 0 and 1 picked at random.

For the nongray case, the wavelength of emission from a source is determined according to the polynomial description proposed by Haji-Sheikh[12] and given in the Appendix (Part 1).

The direction of emission or reflection of an energy bundle is defined by the direction vector R_u, whose coordinates are expressed in terms of the azimuthal, φ, and polar, θ, angles. The two angles are determined by

$$\theta_s = \cos^{-1}(1 - 2R_\theta) \qquad \theta_{surf} = \sin^{-1}\left(\sqrt{R_\theta}\right) \qquad (3)$$

$$\varphi_{s,surf} = 2\pi R_\phi \qquad (4)$$

θ_s is valid for bundle emission from a source (solid angle = 4π), and θ_{surf} is used for a bundle reflected from a surface. The expression for the azimuthal angle is valid for both a source and a surface.

The position of a bundle in space is defined in terms of its origin and the direction vector, R_u, by

$$x = x_s + x_u t \qquad y = y_s + y_u t \qquad z = z_s + z_u t \qquad (5)$$

where t is a positive value.

For a bundle to hit one of the planar surfaces defined by

$$Ax + By + Cz + D = 0 \qquad (6)$$

where A, B, C, and D are constants, the following equation must be fulfilled:

$$A(x_s + x_u t) + B(y_s + y_u t) + C(z_s + z_u t) + D = 0 \qquad (7)$$

Equation (7) is used to solve for t, which is then substituted into Eq. (5) to compute the bundle position. A bundle intersects a surface if its coordinates are within the bounds of the specified surface. Similarly, further planar surfaces with differing shapes can also be considered if their geometries are well defined.

Among the bundles impinging on a surface, a fraction α is absorbed and the rest of the bundles are reflected from the surface. Absorption of a bundle is determined by comparing the surface absorptivity at a given wavelength, α_λ, with a randomly generated number, R_α. The condition of absorption of an energy bundle by a surface is given by

$$R_\alpha \le \alpha_\lambda \qquad (8)$$

In this case, a new bundle is generated and its history is traced using Eqs. (2) through (8). If a bundle is reflected on a sur-

face, a new direction for the bundle in the enclosure is chosen and the bundle history is traced using Eqs. (3) through (8).

In the present work, the exchange factor is defined as the fraction of diffuse radiation emitted by a discrete source, s, that is absorbed by a surface, i, either directly or after multiple reflections on the surfaces

$$dF_{s-i} = \frac{\text{number of photons leaving s} \rightarrow \text{i (direct \& indirect)}}{\text{total number of photons leaving s}} \tag{9}$$

The total exchange factor F_{s-i} between a source s and a surface, i, is calculated by integrating Eq. (9) over a large number of energy bundles emitted by source s:

$$F_{s-i} = \left(\frac{NA_{s-i}}{NB} \right)_{NB>>1} \tag{10}$$

Finally, the total exchange factor F_{sg-i} between a linear succession of sources and any surface, i, in the enclosure is obtained by summing up all factors F_{s-i} given by Eq. (10) over the number of all sources making up the linear surface.

RESULTS AND DISCUSSION

In the following paragraphs, three cases with increasing complexity are presented and solved using the computer program. The latter serves as an exercise in an undergraduate course in heat and mass transfer. The lessons learned through each solved case include closed- and open-ended questions and require students to use thinking skills, in accordance with Bloom's Taxonomy.[4] The dimensions of the system geometry and the values of many other parameters can be changed at will by the students through an input file (see description of the code usage in the Appendix, Part 2). The parameters pertain to enclosure, blocking surface, and heating wire dimensions; to blocking surface and heating wire locations; and to the properties of the surfaces.

In Case 1, a black enclosure without the obstructing surface is considered, and a test problem is presented. The test problem also has an analytical solution so students can verify the computations for themselves. Case 2 concerns radiative exchange in a diffuse-gray enclosure containing a diffuse-gray obstructing surface. Unless otherwise stated, all surfaces are assumed to have the same absorptivity, α, of 0.45. Case 3 is similar to Case 2, but all surfaces are treated as nongray, *i.e.*, with wavelength-dependent absorptivities. In the present study, all calculation results for Cases 2 and 3 correspond to a number of energy bundles per single source of 10^6. Moreover, thermal radiation is emitted by a linear succession of sources, with a sample size of 500 sources, mimicking a heating wire. The sources are considered to lie between segment ends of dimensionless coordinates ($x_{sg}/X=0.5$, $y_{sg}/X=0.25$) and ($x_{sg}/X=0.5$, $y_{sg}/X=0.75$).

Case 1

The Monte Carlo program has been tested for the case of an enclosure whose six walls are black. For the sake of simplification, in the example presented here heat radiation is emitted from a single source placed at position ($x_s/X=0.5$, $y_s/X=0.5$, $z_s/X=0.5$) coinciding with the center of the black enclosure. Results for this example are shown in Figures 2 and 3.

Figure 2 illustrates the calculated view factors between the source and the six surfaces of the enclosure as a function of the size of the sample of energy bundles. By so doing, the students get a better feel for the Monte Carlo method by observing its accuracy as a function of sample size. As the total number of emitted bundles increases, the calculated values of the view factors tend directly to or oscillate about the exact solution corresponding to $F_{s-1} = F_{s-2} = F_{s-3} = F_{s-4} = F_{s-5} = F_{s-6} = 1/6$ for surface 1 through surface 6, respectively. One point worthy of notice in Figure 2 is that accuracy in the calculated view factors is improved only for a bundle sample size of 10^5 and larger. For the latter bundle sample size, the computed view factors are: $F_{s-1} = 0.1662$, $F_{s-2} = 0.1664$, $F_{s-3} = 0.1667$, $F_{s-4} = 0.1670$, $F_{s-5} = 0.1667$, $F_{s-6} = 0.1669$, for surface 1 through surface 6, re-

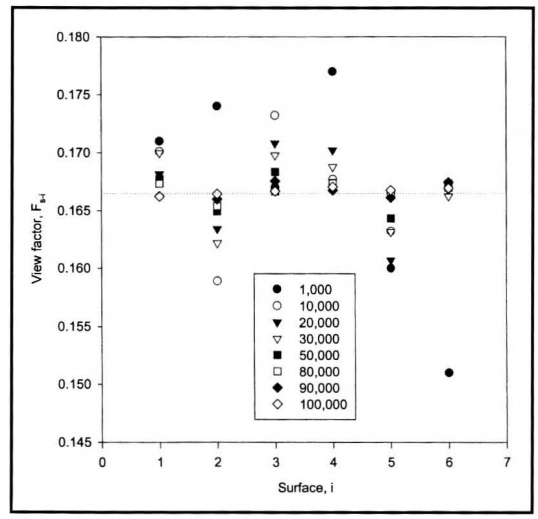

Figure 2. *Calculated view factors of the different black surfaces as a function of the number of emitted bundles (in the inset). The dotted line represents the analytical solution.*

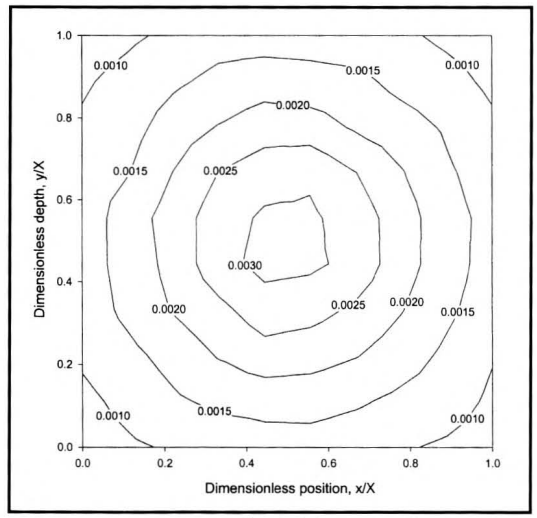

Figure 3. *Contour plot of the view factor over the black surface of the bottom wall.*

spectively, with a maximum relative error of 0.3%. In Figure 3, a typical contour plot depicting the distribution of the local view factor is shown for surface 3 (bottom wall). For all surfaces, the view factor reaches its largest value around the center of a surface, which is closest to the source, and decreases toward surface edges.

Case 2

In this case, the walls of the enclosure and the obstructing surface are considered diffuse and gray. The center of the obstructing surface, denoted surface 0, coincides with the center of the enclosure. A linear succession of sources is located between the bottom wall of the enclosure and the obstructing surface.

Figure 4 shows the dependence of the calculated exchange factors of the surfaces on the height, z_{sg}/X, of the linear source when all surfaces are assumed to have an absorptivity of 0.45. As the linear source is moved upward from the bottom wall, the magnitude of the exchange factor increases from ~0.09 to ~0.22 for the obstructing surface, and decreases from ~0.34 to ~0.20 for the bottom wall. This result is expected since the exchange factor is inversely proportional to the square of the distance between two interacting bodies. For the remaining surfaces, *i.e.,* the lateral surfaces and surface 1 (top wall), the value of the calculated exchange factor slightly increases as the linear source is raised to a dimensionless height of 0.3, then the exchange factor slightly decreases with increasing the height of the linear source (see Figure 4). The results also show that the exchange factors of surface 2 and surface 4 are equal in magnitude (as well as those of surfaces 5 and 6). This is because of the symmetry they exhibit relative to the obstructing surface and linear source (the same goes for surfaces 5 and 6).

The distributions of the calculated exchange factor, corresponding to a height of the linear source of 0.1, on the obstructing surface and surfaces 1 and 2, are presented in Figures 5a,b,c, respectively. It is interesting to note that the exchange factor was found to be at its maximum value near the center of the top surface, where the central areas do not face the source directly, as can be seen in Figure 5b. One of the reasons for this distribution pattern is that multiple bundle reflections on the surfaces were needed for the exchange factors to fulfill the summation relation. For instance, the sum of the calculated exchange factors for all surfaces is higher

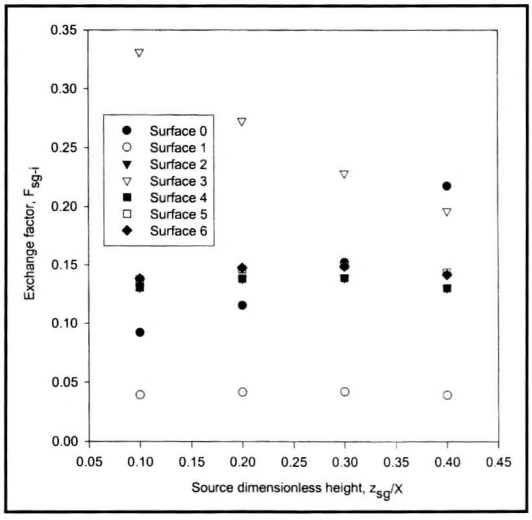

Figure 4. *Dependence of exchange factors on the height of the linear source for the different surfaces (in the inset).*

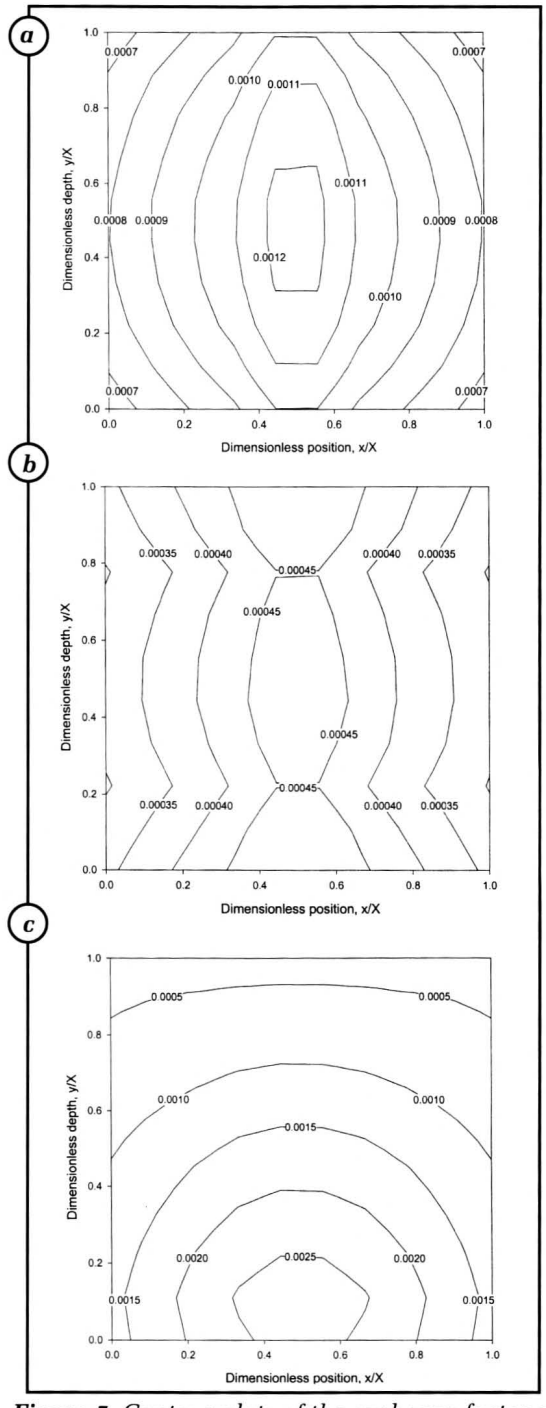

Figure 5. *Contour plots of the exchange factor over surface 0 (a), surface 1 (b), and surface 2 (c).*

than 99.95% only after four, six, and twelve reflections before terminating a bundle for a surface absorptivity, a, of 0.70, 0.45, and 0.20, respectively. Figure 6 illustrates the effect of surface absorptivity on the calculated exchange factors of the different surfaces. A decrease in surface absorptivity induces an increase (decrease) in the exchange factor for the top wall (bottom wall). A low surface absorptivity implies that a bundle has a good chance of being reflected upon impinging on a surface rather than being immediately absorbed. That is, a bundle can travel a long distance within the enclosure and reach remote areas before it is terminated.

Case 3

In this case, the walls of the enclosure and the obstructing surface are considered nongray and their spectral absorptivity is assumed to follow the simple distribution shown in Figure 7a (this is a good approximation for some important metals.[13]) The MC program has a routine to account for the wavelength dependence of surface absorptivity. Thermal radiation emission is due to a linear succession of sources with the same characteristics as those corresponding to the results of Case 2, and with $z_{sg}/X = 0.1$.

Figure 7b illustrates the calculated exchange factors of the different surfaces in the enclosure as a function of the splitting (cut-off) wavelength λ_{sp}. The magnitudes of the exchange factors vary sensibly as λ_{sp} is increased for the top wall (F_{sg-1} varies from ~0.08 to ~0.04) and bottom wall (F_{sg-1} varies from ~0.26 to ~0.33), but only slightly for the obstructing surface and lateral walls of the enclosure. As can be seen in Figure 7b, the calculated exchange factors are insensitive to λ_{sp} for values of the latter higher than 4.0 μm and become comparable in magnitude to exchange factors corresponding to the gray-body case (see Figure 6, case with $\alpha = 0.45$).

CONCLUSIONS

This paper has discussed calculation of the view/exchange factor in an enclosure, with three problems related to different aspects of thermal radiation, using the MC method. The methodology has been presented in a simple and intuitive way so that no additional background in statistics is required. It provides new mathematical concepts that, generally, are not taught in courses on thermal radiation. The computer program is modular, very robust, and easy to use as an educational tool in the analysis of radiation problems. In the future, the author intends to make an executable JAVA version of the package available on-line to potential users.

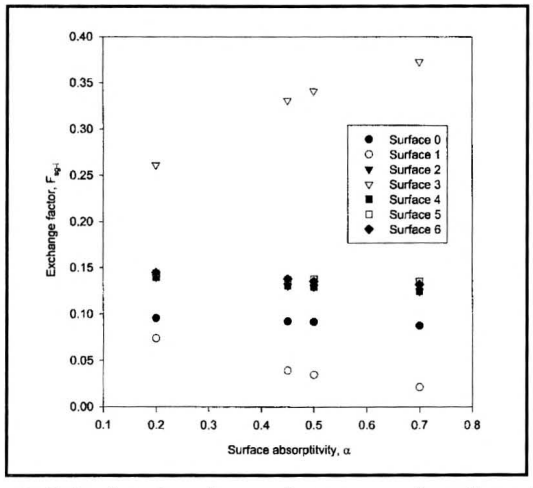

Figure 6. *Calculated exchange factors as a function of surface absorptivity for $Z_{sg}/X = 0.1$. The different surfaces are indicated in the inset.*

ACKNOWLEDGMENT

The author thanks the undergraduate students who helped in implementing and testing the computer program.

NOMENCLATURE

A,B,C,D	constants defining a plane
D_{1-5}	coefficients of inverse probability function, μm.K
E	emissive power, $W/m^2/\mu m$
F	view factor; exchange factor
NB,NA	number of emitted bundles; number of absorbed bundles
R	cumulative distribution function; random number in range 0-1; direction unit vector

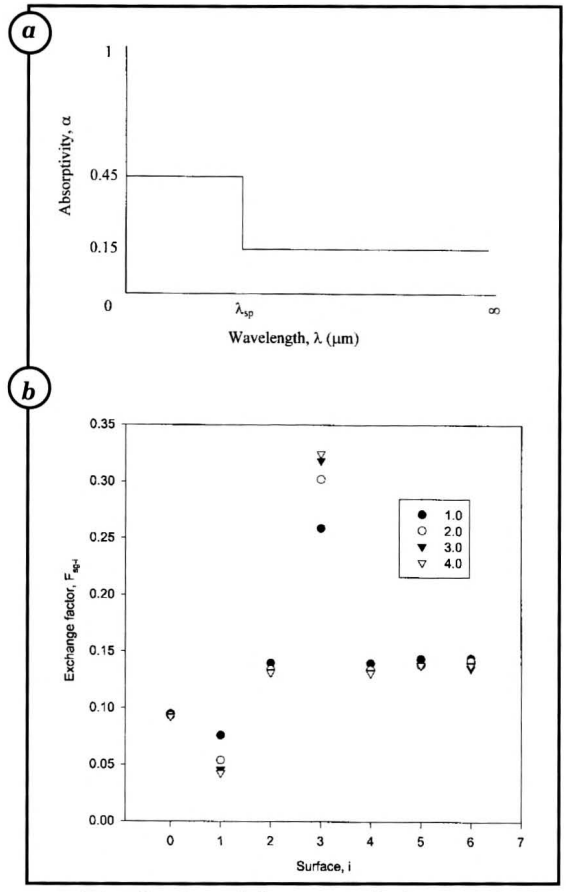

Figure 7. *Distribution of the spectral absorptivity for Case 3 (a), and variation of exchange factors of the different surfaces with the splitting wavelength in the inset (b).*

T,t absolute temperature of emitting source, K; length of bundle
X,Y,Z dimensions of enclosure, m
x,y,z Cartesian system of coordinates; bundle Cartesian coordinates, m

Greek Symbols

α surface absorptivity
θ angle to normal; polar angle
φ azimuthal angle
λ wavelength of emission, μm

Subscripts

i,s surface i, source s
sp,sg splitting, segment
surf surface
u unit
s-i from source s to surface i
sg-i from segment to surface i
λ at a given wavelength
1,2 end-points of linear source

REFERENCES

1. Carnahan, B. (Ed.) *Computers in Chemical Engineering Education* CACHE, Austin, TX (1996)
2. White, S.R., and G.M. Bodner, "Evaluation of Computer Simulation Experiments in a Senior-Level Capstone ChE Course," *Chem. Eng. Ed.*, **33**(1), 34 (1999)
3. Thompson, K.E., "Teaching PDEs to Undergraduates: Overcoming Conceptual and Computational Barriers," *Chem. Eng. Ed.*, **34**(2), 146 (2000)
4. Bloom, B.S., (Ed.), *Taxonomy of Educational Objectives: The Classification of Educational Goals. Handbook 1: Cognitive Domain,* David McKay, Co., New York, NY (1956)
5. Feingold, A., "Radiant-Interchange Configuration Factors Between Various Selected Plane Surfaces," *Proc. R. Soc. London,* **292**, 51 (1966)
6. Howell, J.R., *A Catalog of Radiation Configuration Factors,* McGraw-Hill, New York, NY (1982)
7. Chung, T.J., and J.Y. Kim "Radiation View Factors by Finite Elements," *ASME J. Heat Trans.,* **104**, 792 (1982)
8. Ambirajan, A., and S.P. Venkanteshan, "Accurate Determination of Diffuse View Factors Between Planar Surfaces," *Int. J. Heat Mass Trans.,* **36**, 2203 (1993)
9. Rammohan, V., and V.M.K. Sastri, "Efficient Evaluation of Diffuse View Factors for Radiation," *Int. J. Heat Mass Trans.,* **39**, 1281 (1996)
10. Haines, E., "Essential Ray Tracing Algorithms," in *An Introduction to Ray Tracing,* A. Glassner, ed., Academic Pres, New York, NY; pp 33-77 (1989)
11. Modest, M.F., *Radiative Heat Transfer,* McGraw-Hill, New York, NY (1993)
12. Haji-Sheikh, A., "Monte Carlo Methods," in *Handbook of Numerical Heat Transfer,* W.J. Minkowycz, E.M. Sparrow, G.E. Schneider, and R.H. Pletcher, eds., John Wiley & Sons, New York NY; pp 673-722 (1988)
13. Brewster, M.Q., *Thermal Radiative Transfer and Properties,* John Wiley & Sons, New York, NY; Chapter 2 (1992) ❐

APPENDIX

Part 1. For the nongray case, the wavelength of emission from a source was determined as follows:[12]

$$\lambda T = D_1 + D_2 R_\lambda^{1/8} + D_3 R_\lambda^{1/4} + D_4 R_\lambda^{3/8} + D_5 R_\lambda^{1/2} \quad \text{when } 0.0 < R_\lambda < 0.1$$

$$\lambda T = D_1 + D_2 R_\lambda + D_3 R_\lambda^2 + D_4 R_\lambda^3 + D_5 R_\lambda^4 \quad \text{when } 0.1 < R_\lambda < 0.9$$

$$\lambda T = \left\{ 15.2886 \times 10^{10} / \left[D_1 R_{-\lambda} + D_2 R_{-\lambda}^2 + D_3 R_{-\lambda}^3 + D_4 R_{-\lambda}^4 \right] \right\}^{1/3} \quad \text{when } 0.9 < R_\lambda < 1.0$$

with $R_{-\lambda} = 1 - R_\lambda$, and T= temperature of emitting source.

The coefficients for $\lambda T = f^{-1}(R_\lambda)$ given above are summarized in the table below (λT in μm.K)

Range of R_λ	*D_1*	*D_2*	*D_3*	*D_4*	*D_5*
0.0 - 0.1	503.274	230.243	5863.85	-10759.6	8723.14
0.1 - 0.4	1560.84	7603.61	-15540.1	31257.7	-20844.8
0.4 - 0.7	2846.63	-4430.38	27936.0	-41041.9	25960.9
0.7 - 0.9	345197	-1828567	3674856	-3284391	1108939
0.9 - 0.99	1.2	9.476	-44.84	156.9	-
0.99 - 1.0	1.10064	16.8148	-183.445	890.699	-

Part 2. Flowchart for MC calculation of radiation view/exchange factors. Data pertaining to the geometry and dimensions of the enclosure and obstructing surface, optical properties and temperatures of the surfaces in the enclosure, heating source location and temperature, number of bundles per photon, physical constants, and preset calculation tolerances are needed as input to the computer program. All data pertaining to length and position are expressed in absolute quantities. The input file interfaces between the user and the computer package, and several output files are obtained upon execution of the code. The program was written in C++ using Microsoft Visual Studio, and the output files, in .txt format, are readily transferable to SigmaPlot, a statistics and graphics software from SPSS, Inc., for further processing.